Atmos. Chem. Phys. Discuss., https://doi.org/10.5194/acp-2017-699
Manuscript under review for journal Atmos. Chem. Phys.
Discussion started: 10 August 2017

Atmospheric Chemistry and Physics Discussions

Modeling the partitioning of organic chemical species in cloud phases with CLEPS (1.1)

Clémence Rose[1], Nadine Chaumerliac[1], Laurent Deguillaume[1], Hélène Perroux[1], Camille Mouchel-Vallon[1,a], Maud Leriche[2], Luc Patryl[3], Patrick Armand[3]

[1]Université Clermont Auvergne, CNRS Laboratoire de Météorologie Physique, F-63000 Clermont-Ferrand, France

[2]Université de Toulouse, UPS, CNRS, Laboratoire d'Aérologie, 31400 Toulouse, France

[3]CEA, DAM, DIF, F-91297 Arpajon, France

[a]Now at: National Center for Atmospheric Research, Boulder, Colorado, USA

Correspondence to: N. Chaumerliac (N.Chaumerliac@opgc.univ-bpclermont.fr) and L. Deguillaume (l.deguillaume@opgc.univ-bpclermont.fr)

Abstract. The new detailed aqueous phase mechanism Cloud Explicit Physico-chemical Scheme (CLEPS 1.0), which describes the oxidation of isoprene-derived water-soluble organic compounds, is coupled with a warm microphysical module simulating the activation of aerosol particles into cloud droplets. CLEPS 1.0 was then extended to CLEPS 1.1 to include the chemistry of the newly added di-carboxylic acids dissolved from the particulate phase. The resulting coupled model allows for predicting the aqueous phase concentrations of chemical compounds originating from particle dissolution, mass transfer from the gas phase and in-cloud aqueous chemical reactivity. The aim of the present study was more particularly to investigate the effect of particle dissolution on cloud chemistry. Several simulations were performed to assess the influence of various parameters on model predictions and to interpret long-term measurements conducted at the top of the puy de Dôme (PUY, France) in marine air masses. Specific attention was paid to carboxylic acids, whose predicted concentrations are on average in the lower range of the observations, with the exception of formic acid, which is rather overestimated in the model. The different sensitivity runs highlight the fact that formic and acetic acids mainly originate from the gas phase and have highly variable aqueous-phase reactivity depending on the cloud acidity, whereas C_3-C_4 carboxylic acids mainly originate from the particulate phase and are supersaturated in the cloud.

1 Introduction

Clouds are multiphase systems in which a gas phase, an aqueous phase and aerosol particles coexist and interact. As a result, clouds act as huge chemical reactors where a large variety of both homogeneous and heterogeneous reactions occur. The cloud aqueous phase is the site of reactions that would be hindered or occur with a much slower rate in the gas phase (Herrmann et al., 2015). These reactions may lead to the formation of low volatility species that can in turn modify the physicochemical properties of aerosol particles after the cloud dissipates and further lead to Secondary Organic Aerosol (SOA) formation and aging (Gelencsér and Varga, 2005; Kanakidou et al., 2005; Lim et al., 2010; Sullivan et al., 2016). The accretion and oxidation of organic compounds were identified as competing aqueous processes responsible for the formation and destruction of SOA precursors (Renard et al., 2015). While accretion processes such as oligomerization have been in the scope of numerous recent studies (Ervens et al., 2015), Mouchel-Vallon and co-workers focused on oxidation processes, paying particular attention to the competition between fragmentation and functionalization (Mouchel-Vallon et al., 2017). They developed a protocol to derive CLEPS 1.0 (CLoud Explicit Physicochemical Scheme), a new detailed aqueous-phase oxidation mechanism for low-NO_x conditions able to describe multiple oxidation pathways for each of the considered C_1-C_4

organic species. As a first step, CLEPS 1.0 has been integrated in a box model that takes into account neither aerosol particles nor microphysical processes, and thus only allows for the simulation of idealized cloud events.

This paper describes the coupling between the chemistry model based on CLEPS 1.0 and a bulk two-moment warm cloud microphysical scheme allowing for the simulation of more realistic cloud events. This microphysical scheme predicts both the number concentration and the mixing ratio of cloud droplets and raindrops resulting from the activation of a given aerosol particle spectrum, taking into account the subsequent processes that affect the droplet distribution. The development of such a coupled model offers the opportunity to investigate the impact of aerosol particles on the cloud chemistry (by nucleation scavenging), as well as the importance of cloud microphysical processes in the redistribution of the reactive compounds among the different phases (gas, cloud and rain) (Leriche et al., 2001). It can also document the origin of the chemical species measured in cloud water and rainwater, which is usually not available from measurements (Leriche et al., 2007).

Several physically based parameterizations describing the activation of aerosol particles into cloud droplets are available from the literature. Sectional cloud parcel models provide a physically realistic and internally consistent calculation of particle activation and droplet growth in a rising parcel of air. They are however computationally too expensive to be used with detailed explicit aqueous-phase chemistry such as that described in CLEPS 1.0. The use of parameterizations to estimate the number of activated particles is thus better adapted to this purpose. The most widely used parameterization schemes fall into two families – those based on the work of Abdul-Razzak et al. (1998) and Abdul-Razzak and Ghan (2000) and those following Fountoukis and Nenes (2005). The parameterizations provided in these studies differ by the aerosol size distribution they use and the way they treat the activation process. They have been discussed by Simpson et al. (2014) to demonstrate the effect of activating large particles described by a single lognormal mode simulation and by Ghan et al. (2011), who concluded that all parameterizations performed well under the most common conditions, i.e., when cloud condensation nuclei (CCN) are mainly in the accumulation mode.

In the present study, the activation of aerosol particles into cloud droplets is described using the parameterization from Abdul-Razzak (Abdul-Razzak et al., 1998; Abdul-Razzak and Ghan, 2000) based upon the Köhler theory (Köhler, 1936) and further modified (Abdul-Razzak and Ghan, 2004) to take into account the influence of organic surfactants on the activation process. This last improvement was prompted by the increasing evidence of a significant organic fraction in the chemical composition of aerosol particles (Kanakidou et al., 2005), in particular that of CCN. For instance, a notable amount of organic matter (up to 60% of the total mass) was detected by a cTof-AMS in the CCN measured at the puy de Dôme station (Asmi et al., 2012). Paying more attention to the effect of surfactants on cloud droplet formation follows the global interest that emerged in the literature (McNeill et al., 2013), with a multiplicity of laboratory and field studies dedicated to this research area (Gérard et al., 2016; Nozière et al., 2014), as well as global modeling studies (Prisle et al., 2012).
In addition to their influence on the activation process itself, the chemical properties of aerosol particles also impact the in-cloud aqueous-phase chemistry through the dissolution of soluble species. This last effect makes it possible, in particular, to simulate the chemistry of those species that only originate from particle dissolution, such as transition metals (Deguillaume et al., 2005), or that are usually reported as key constituents of the particulate phase, such as di-carboxylic acids (Chebbi and Carlier, 1996). The coupled model can also provide insights into the processing of these particle-originating organic species in the cloud aqueous phase. To make the most of these opportunities, the oxidation pathways of several additional C_4 di-carboxylic acids was implemented in CLEPS (V1.1) compared to the initial version of the mechanism introduced in Mouchel-Vallon et al. (2017). Succinic, malic, tartric and fumaric/maleic acids were included as they are usually among the major organic compounds measured in aerosol particles in a large variety of environments, including urban (Kawamura and Kaplan, 1987; Kawamura and Yasui, 2005; Kerminen et al., 2000; Limbeck and Puxbaum, 1999; van Pinxteren et al., 2014; Sempére and Kawamura, 1994; Yao et al., 2002), rural (Kerminen et al., 2000; Müller et al., 2005; van Pinxteren et al.,

2014), mountainous (Kawamura et al., 2013; Legrand et al., 2007; Limbeck and Puxbaum, 1999), marine (Kawamura and Sakaguchi, 1999; Mochida et al., 2003) and Arctic (Kawamura et al., 2012) atmospheres.

In this paper, the main features of CLEPS 1.1 are first briefly summarized, and the developments in the chemistry of the newly added particle-originating compounds are introduced. Then, the microphysical module based upon the parameterization of Abdul-Razzak and Ghan (2004) and on a bulk cloud scheme previously used by Leriche et al. (2001) is described. The ability of the coupled model to predict concentrations in the range of those measured during cloud events at the puy de Dôme (PUY) station is finally tested.

2 Model Description

2.1 The multiphase chemistry model – focus on di-carboxylic acids

The recent cloud chemistry model based on the explicit aqueous-phase oxidation mechanism CLEPS 1.0 was first introduced in Mouchel-Vallon et al. (2017), where a detailed description can be found.

In addition to the inorganic chemical scheme previously described in Deguillaume et al. (2004) and in Leriche et al. (2007), CLEPS 1.0 describes the $HO^{\cdot}$ and $NO_3^{\cdot}$ oxidation pathways of $C_{1\text{-}4}$ organic compounds following the methodology developed by Mouchel-Vallon et al. (2017). CLEPS 1.0 relies on recent improvements in the estimation of kinetic and thermodynamic parameters based on Structure-Activity Relationships (SARs) derived from experimental data (Doussin and Monod, 2013; Minakata et al., 2009; Monod and Doussin, 2008; Raventos-Duran et al., 2010). Mouchel-Vallon and co-workers used these SARs 1) to derive the reaction rates or equilibrium constants of species that were not well documented in the literature and 2) to determine, for the first time, the branching ratios and further select the major oxidation pathways with $HO^{\cdot}$ to be included in the mechanism. CLEPS 1.0 was coupled to the gas phase mechanism MCM v3.3.1 (Master Chemical Mechanism) (Jenkin et al., 2015; Saunders et al., 2003), and the exchange between the aqueous and gas phases was accounted for through the kinetic mass transfer theory of stable species following Schwartz (1986).

The whole mechanism, including CLEPS 1.0, MCM v3.3.1 and mass transfer reactions, was integrated in a box model based on DSMACC (Dynamically Simple Model for Atmospheric Chemical Complexity) (Emmerson and Evans, 2009) and using the KPP (Kinetic PreProcessor) (Damian et al., 2002) modified to consider an aqueous phase. The TUV 4.5 radiative transfer model (Madronich and Flocke, 1997) initially set up in DSMACC and dedicated to the calculation of photolysis rates in the gas phase was adapted to include aqueous-phase photolysis reactions.

For each of the chemical species included in the model, the set of differential equations describing the time evolution of the concentrations in the gas phase and in the cloud aqueous phase is written as:

$$\frac{dC_g}{dt} = P_g - DE_g C_g + \frac{k_{t_{cw}} C_{cw}}{H_{eff} RT} - q_{cw} k_{t_{cw}} C_g \quad (1)$$

$$\frac{dC_{cw}}{dt} = P_{cw} - DE_{cw} C_{cw} + q_{cw} k_{t_{cw}} C_g - \frac{k_{t_{cw}} C_{cw}}{H_{eff} RT} \quad (2)$$

In Eqs. (1) and (2), the subscripts g and cw refer to the gas phase and cloud aqueous phase, respectively, so that C_g and C_{cw} are, respectively, the gaseous and aqueous chemical concentrations (molec cm^{-3}), P_g and P_{cw}, and DE_g and DE_{cw} are, respectively, the gaseous and aqueous chemical production and destruction terms (cm^{-3} s^{-1} and s^{-1}, respectively), H_{eff} is the Henry's law effective constant (M atm^{-1}), q_{cw} is the cloud liquid water content (vol/vol) and R = 0.08206 atm M^{-1} K^{-1}. $k_{t_{cw}}$ is the inverse of the sum of the characteristic times for gaseous diffusion and interfacial mass transport (Schwartz, 1986), expressed as:

$$k_{t_{cw}} = \left(\frac{r^2}{3D_g} + \frac{4r}{3\bar{v}\alpha}\right) \quad (3)$$

where r is the droplet radius in cm, D_g is the gaseous diffusion coefficient ($cm^2\ s^{-1}$), and $\bar{v}$ and α are respectively the mean quadratic speed in cm s^{-1} and the accommodation mass coefficient of the species. The effective Henry's law constant accounts for the dissociation or hydration of soluble gases in the aqueous phase, and its determination is thus based upon the use of dissociation and/or hydration constants. These last parameters, together with the Henry's law constant and the accommodation mass coefficient, are prescribed from laboratory measurements or estimated from SARs (Mouchel-Vallon et al., 2017 and references therein). Eqs. (1) and (2) are solved with a Rosenbrock solver, previously reported to be the most accurate in the frame of multiphase chemistry modeling (Djouad et al., 2002, 2003). The pH of the droplets is calculated from the concentration of H^+, which is explicitly treated in equilibrium reactions solved kinetically with forward and backward reactions.

Developments were made on CLEPS 1.0 to describe the oxidation of di-carboxylic acids which mainly originate from the particle phase and can possibly act as CCN. Di-carboxylic acids are among the best quantified in-particle organic species, though they usually account for only a small fraction of the total organic mass (Saxena and Hildemann, 1996), up to 16% in remote marine aerosols (Kawamura and Sakaguchi, 1999). While monocarboxylic acids can display concentrations increased by several orders of magnitude in the gas phase compared to the particulate concentrations (Chebbi and Carlier, 1996), di-carboxylic acids are in contrast likely to dominate in the particulate phase as a result of their lower vapor pressure (Ludwig and Klemm, 1988). The presence of low molecular weight di-acids (such as oxalic acid) in the gas phase was however reported, and might be favored under conditions of elevated temperature, low relative humidity and low aerosol pH (Clegg et al., 1996; Kawamura and Kaplan, 1987).

Due to their solubility properties, di-carboxylic acids influence the ability of aerosol particles to act as CCN (Saxena and Hildemann, 1996; Shulman et al., 1996) and, in turn, impact the Earth's radiative budget and climate. Surface tension depression by water soluble di-carboxylic acids in solution was reported by McNeill et al. (2013), involving C_3 and C_4 compounds such as malonic, malic, succinic and maleic acids. Enhanced reduction effects on the surface tension were observed with the increasing carbon chain length and concentration. Paying particular attention to mixed ammonium sulfate and organic acids (including malonic acid) particles, Abbatt et al. (2005) also showed that the CCN efficiency of the mixed inorganic-organic particles was likely to be significantly modified by solubility effects compared to that of pure inorganic particles. Di-carboxylic acids are of particular interest in the frame of the present study since they can be used as tracers to follow the processing of the whole particulate soluble organic fraction (Ervens et al., 2011), although they only represent a few percent of this soluble organic matter (Legrand et al., 2007).

In this context, the oxidation pathways of succinic, malic, tartric and fumaric/maleic acids were implemented in the model following the protocol described by Mouchel-Vallon et al. (2017). 65 oxidation reactions and 37 equilibria, were thus newly included in CLEPS and are reported in details in the tables of the **Supplementary Material**. These C_4 di-carboxylic acids, are, together with oxalic (C_2), malonic (C_3) and glutaric (C_5, not treated in CLEPS) acids, among the main organic compounds measured in aerosol particles. Regardless of the site or the season, oxalic acid is always reported to be the most abundant di-carboxylic acid, usually followed by malonic and succinic acids (Chebbi and Carlier, 1996; Mader et al., 2004). For example, these three compounds account on average for 60 to 80% of the diacids measured at European continental sites (Legrand et al., 2007; Müller et al., 2005; van Pinxteren et al., 2014), while oxalic acid alone can represent more than 60% of these diacids (Legrand et al., 2007).

Sources of di-carboxylic acids include biogenic and anthropogenic emissions, as well as the photochemical transformations of precursors (Chebbi and Carlier, 1996; Dabek-Zlotorzynska and McGrath, 2000). While no primary sources have been

reported so far for malic and tartric acids, oxalic, malonic, succinic and glutaric acids were measured in motor exhaust (Kawamura and Kaplan, 1987). The last three were also observed in wood burning plumes (Rogge et al., 1998). However, a major fraction of the di-carboxylic acids is likely to be produced by the photochemical oxidation of organic precursors in the atmosphere, occurring both in the gas and aqueous phases (van Pinxteren et al., 2014).

2.2 Description of the microphysical scheme

The two-moment warm microphysical scheme predicts the number concentration of cloud droplets and raindrops as well as the mixing ratios of cloud water and rainwater using log-normal distributions (Caro et al., 2004), as previously done by Leriche et al. (2007). Only the activation of aerosol particles has been updated to account for the influence of organic surfactants (Abdul-Razzak and Ghan, 2004).

2.2.1 Activation of aerosol particles into cloud droplets

The activation of aerosol particles into cloud droplets is described according to the work of Abdul-Razzak et al. (1998) and Abdul-Razzak and Ghan (2000, 2004). These parameterizations are all based upon the Köhler theory (Köhler, 1936) and aim at finding the maximum supersaturation on each model time step considering the physico-chemical properties of the aerosol. The Köhler equation describes the balance of water vapor pressure over a growing droplet resulting from two competitive effects: the effects of curvature and surface tension on the one hand (Kelvin term) and the hygroscopicity of the solute on the other (Raoult term). It is assumed in Köhler theory that particles stay in equilibrium with the local supersaturated water vapor until activated as CCN, and thus react instantly to any supersaturation change. Such an assumption might be inexact and lead to overestimating the droplet number concentrations under certain conditions where kinetic limitations on droplet growth exist (Nenes et al., 2001). However, when compared with the predictions from an adiabatic parcel model, the parameterizations from Abdul-Razzak et al. (1998) and Abdul-Razzak and Ghan (2000) were reported to well predict the cloud activation for updraft velocities higher than 0.5 m s^{-1} and particle number concentrations lower than 500 cm^{-3} (Phinney et al., 2003).

While the efficiency of the Köhler equation to model the CCN behavior of soluble inorganic compounds is recognized, it might be less efficient in predicting the activation of less hygroscopic particles, such as organic or mixed organic-inorganic particles. In the last parameterization provided by Abdul-Razzak and Ghan (2004), a modified version of the Köhler theory is used to represent the influence of organic surfactants on aerosol activation. Both recent experimental laboratory and field studies have shown that the presence of such compounds may modify the CCN activity of aerosol particles as a function of the surfactant type and ambient conditions (McNeill et al., 2013).

The treatment of these effects in the parameterization of the activation process is fully described in Abdul-Razzak and Ghan (2004), and only briefly recounted here. Following Shulman et al. (1996), the contributions of inorganic salts and organic surfactants are expressed as a sum in the Raoult term of the modified Köhler theory, assuming additive effects on the vapor pressure. In parallel, the decrease of the surface tension (Kelvin term) is estimated as a function of the surfactant molar concentration using Szyskowski's empirical formula (Szyskowski, 1908). Following Li et al. (1998) and earlier work by Corrin and Harkins (1947), the formation of micelles at the droplet surface occurring in the case of high surfactant concentrations is also accounted for in the present study.

The aerosol particles to be potentially activated are considered in the model in the form of a multi lognormal-mode size distribution, as required by Abdul-Razzak and Ghan (2004):

$$\frac{dN_{ap}}{d\ln d_{ap}} = \sum_{i=1}^{n} \frac{N_{api}}{\ln \sigma_i \sqrt{2\pi}} \exp\left[-\frac{ln^2\left(\frac{d_{ap}}{d_{mi}}\right)}{2\, ln^2 \sigma_i}\right] \quad (4)$$

where n is the number of modes, N_{ap} is the total number concentration of aerosol particles, N_{api} is the number concentrations of aerosol particles in mode i; d_{mi} is the median diameter of the log-normal distribution for mode i; σ_i is the geometric standard deviation of the log-normal distribution of mode i and d_{ap} is the diameter of the aerosol particles.

At each time step, the number of newly nucleated droplets ($\left(\frac{\partial N_{cw}}{\partial t}\right]_{NUC}$) and the corresponding cloud water mixing ratio are derived from the activated fraction of particles in each mode. To avoid unrealistic supersaturations, the particle size distribution is maintained constant throughout the simulation, while the maximum particle number and mass to be further activated are constrained in each mode with the initial number and mass concentrations. The aqueous concentrations of particle-originating chemical species are calculated in the droplet from the soluble fraction of the activated aerosol mass prescribed from measurements.

2.2.2 Evolution of the cloud droplet distribution - rain formation

The dynamical framework of the model is an air parcel that mimics the rising of a moist orographic parcel. The evolution of the cloud, including the appearance of rain, is described according to Berry and Reinhardt's parameterization (Berry and Reinhardt, 1974a,b,c,d), as previously done in Leriche et al. (2001), where more details can be found regarding the use of the parameterization. The resulting two-moment scheme includes the condensation/evaporation of cloud water and rainwater (CO), the autoconversion of cloud into rain (AU), the accretion of cloud droplets on larger drops (AC), the self-collection of raindrops between themselves (SC), the partial evaporation of cloud droplets and rain drops (EV) and the sedimentation (SED) of raindrops. This leads to the following set of equations for water vapor (subscript *v*), cloud water (subscript cw) and rainwater (subscript rw).

$$\frac{dq_v}{dt} = -\frac{\partial q_{cw}}{\partial t}\Big]_{NUC} - \frac{\partial q_{cw}}{\partial t}\Big]_{CO} - \frac{\partial q_{rw}}{\partial t}\Big]_{CO} + \frac{\partial q_{cw}}{\partial t}\Big]_{EV} + \frac{\partial q_{rw}}{\partial t}\Big]_{EV} \quad (5)$$

$$\frac{dN_{cw}}{dt} = \frac{\partial N_{cw}}{\partial t}\Big]_{NUC} - \frac{\partial N_{cw}}{\partial t}\Big]_{AU} - \frac{\partial N_{cw}}{\partial t}\Big]_{AC} - \frac{\partial N_{cw}}{\partial t}\Big]_{EV} \quad (6)$$

$$\frac{dq_{cw}}{dt} = \frac{\partial q_{cw}}{\partial t}\Big]_{NUC} + \frac{\partial q_{cw}}{\partial t}\Big]_{CO} - \frac{\partial q_{cw}}{\partial t}\Big]_{AU} - \frac{\partial q_{cw}}{\partial t}\Big]_{AC} - \frac{\partial q_{cw}}{\partial t}\Big]_{EV} \quad (7)$$

$$\frac{dN_{rw}}{dt} = \frac{\partial N_{rw}}{\partial t}\Big]_{AU} - \frac{\partial N_{rw}}{\partial t}\Big]_{SC} - \frac{\partial N_{rw}}{\partial t}\Big]_{SED} - \frac{\partial N_{rw}}{\partial t}\Big]_{EV} \quad (8)$$

$$\frac{dq_{rw}}{dt} = \frac{\partial q_{rw}}{\partial t}\Big]_{AU} + \frac{\partial q_{cw}}{\partial t}\Big]_{CO} + \frac{\partial q_{rw}}{\partial t}\Big]_{AC} - \frac{\partial q_{rw}}{\partial t}\Big]_{SED} - \frac{\partial q_{rw}}{\partial t}\Big]_{EV} \quad (9)$$

The cloud droplet and raindrop spectra are both represented by single log-normal distributions. The geometric standard deviation of the cloud droplet size distribution is fixed to 0.28 and 0.15 for maritime and continental air masses respectively, while it remains fixed at 0.547 for the raindrop size distribution regardless of the air mass type (Chaumerliac et al., 1987). In contrast, the median diameters of the distributions are calculated at each time step from the respective water mixing ratios.

2.3 Coupling the chemistry model with the microphysical scheme

The initial set of differential equations (1) and (2) has been completed to extend the chemical reactivity and mass transfer to raindrop species (subscript rw):

$$\frac{dC_g^i}{dt}\Big]_{chem} = P_g - D_g C_g + \frac{k_{t_{cw}} C_{cw}}{H^* RT} - q_{cw} k_{t_{cw}} C_g + \frac{k_{t_{rw}} C_{rw}}{H^* RT} - q_{rw} k_{t_{rw}} C_g \quad (10)$$

$$\frac{dC_{cw}^i}{dt}\Big]_{chem} = P_{cw} - D_{cw} C_{cw} + q_{cw} k_{t_{cw}} C_g - \frac{k_{t_{cw}} C_{cw}}{H^* RT} + T_{ap} \quad (11)$$

$$\left.\frac{dC_{rw}^{i}}{dt}\right]_{chem} = P_{rw} - D_{rw}C_{rw} + q_{rw}k_{t_{rw}}C_g - \frac{k_{t_{rw}}C_{rw}}{H^*RT} \quad (12)$$

The term T_{ap} has been introduced in Eq. (10) to take into account the inputs related to the dissolution of the particulate matter in the cloud droplet (hereafter referred to as particle-to-cloud transfer). The rates of change of the chemical concentrations described by Eqs. (10), (11) and (12) are, with the exception of the particle-to-cloud transfer, driven by the chemical reactivity and mass transfer, which are predicted in the chemistry model itself. They will thus hereafter be traced by the subscript $chem$ to distinguish from the variations caused by the microphysical conversions related to some of the processes initially accounted for in the microphysical module (see Sect. 2.2.2):

$$\frac{dC_g^i}{dt} = \left.\frac{dC_g^i}{dt}\right]_{chem} \quad (13)$$

$$\frac{dC_{cw}^{i}}{dt} = \left.\frac{dC_{cw}^{i}}{dt}\right]_{chem} - \left.\frac{dC_{cw}^{i}}{dt}\right]_{AU} - \left.\frac{dC_{cw}^{i}}{dt}\right]_{AC} \quad (14)$$

$$\frac{dC_{rw}^{i}}{dt} = \left.\frac{dC_{rw}^{i}}{dt}\right]_{chem} + \left.\frac{dC_{rw}^{i}}{dt}\right]_{AU} + \left.\frac{dC_{rw}^{i}}{dt}\right]_{AC} - \left.\frac{dC_{rw}^{i}}{dt}\right]_{SED} \quad (15)$$

For any of the microphysical processes included in the previous equations (autoconversion, accretion, sedimentation), the corresponding rate of change can be written in the form of a proportionality relationship:

$$\left.\frac{dC_{yw}^{i}}{dt}\right]_{Y} = \left.\frac{C_{yw}^{i}}{q_{yw}}\frac{dq_{yw}}{dt}\right]_{Y} \quad (16)$$

where the subscript $y \in \{c, r\}$ either describes cloud or rainwater and the subscript Y either refers to autoconversion, accretion or sedimentation. No term is added for condensation/evaporation because the balance between the gas phase and the aqueous phase is done by the kinetic mass transfer terms.

An overview of the coupled model is provided in **Fig. 1**, which highlights the developments performed in the frame of the present work. Many of these developments have to do with the appearance of rainwater in the model, including the duplication of the aqueous oxidation scheme, reactions rates, equilibria and mass transfer, as well as the implementation of new user routines to describe the cloud-to-rain transfer of chemical species (related to autoconversion and accretion processes) and the sink for rain species (related to the sedimentation process). An additional user routine was also developed to treat the particle-to-cloud transfer.

In practice, the microphysical scheme module is first run to provide a set of look-up tables. These tables contain the time evolution of meteorological variables (temperature, pressure and relative humidity), cloud and rain microphysics (mixing ratio, droplet diameter), and microphysical conversion rates as well as the chemical concentration of the species involved in the particle-to-cloud transfer. In a second stage, the values compiled in the tables are interpolated in time and read as input data by the chemistry model to solve Eqs. (13), (14) and (15) at each time step and for each of the chemical species considered in the model.

2.4 Initialization of the coupled model

The ability of the coupled model to predict cloud chemistry, including the processing of organic compounds and to reproduce concentrations in the range of those measured during real cloud events was tested on an ideal case study. In the frame of the present work, we have chosen to focus on a particular aspect of the developments previously introduced, namely, the particle-to-cloud-transfer of chemical species. A non-precipitating orographic cloud representative of those observed at the puy de Dôme (PUY) station (France, 1465 m a.s.l.) (Freney et al., 2011) was simulated from the temperature

and altitude time profiles shown in **Fig. 2** to minimize possible meteorological and rain effects. The understanding of these last effects will be left for further dedicated studies. More complex air mass back-trajectories, such as those provided by a three dimensional model and used by Leriche et al. (2007) might be used in that case.

The initial gas phase composition was derived from the low-NO_x situation described by McNeill et al. (2012) and is representative of the conditions encountered at the PUY station (Freney et al., 2011). The emission and deposition rates used in the present work are derived from Mouchel-Vallon et al. (2017) and are reported in **Table 1.** Following the same procedure as Mouchel-Vallon et al. (2017), a gas chemistry spin-up simulation was run for 4.5 days until the appearance of the cloud at noon on the 5th day and the start of the aqueous-phase chemistry.

The physical characteristics of a typical aerosol measured at the PUY station were derived from Sellegri et al. (2003). These data was used to initialize the aerosol particle spectrum as previously done in Leriche et al. (2007). The particle size distribution is represented as the sum of four log-normal modes, including an Aitken mode approximately 76 nm, a first accumulation mode approximately 410 nm, a second accumulation mode approximately 660 nm and a coarse mode approximately 2.6 µm. More details on the physical characteristics of these modes (particle number concentration, geometric standard deviation and diameter) can be found in **Table 2**. The aerosol densities and soluble mass fractions are calculated using the chemical composition of the particles and are also reported in **Table 2**.

The chemical composition of the particles was prescribed according to the measurements conducted between February 28th and March 1st 2000 by Sellegri et al. (2003) in a moderately polluted air mass. Particles were sampled using a low-pressure cascade impactor (13-stage ELPI impactor, commercialized by DEKATI Inc) and were further analyzed using ion chromatography. The mass fraction of iron was derived from Particle-Induced X-ray Emission (PIXE). More details on the sampling procedure and data analysis can be found in Sellegri et al. (2003).

The mass distribution of the di-carboxylic acids derived from these measurements is shown in **Fig. S1** in the Supplementary Material. As expected, oxalic acid is the most abundant and the major fraction of the diacids found in the two accumulation modes (0.4 – 1 µm), as previously observed at other continental European sites (Legrand et al., 2007; Müller et al., 2005; van Pinxteren et al., 2014). When comparing these concentrations with those obtained at the PUY station during the CARBOSOL project (Present and Retrospective State of Organic versus Inorganic Aerosol over Europe: Implications for Climate) by Legrand et al. (2007), we found a fair agreement for succinic (this study: 5.98 ng m^{-3}, Legrand et al. (2007): 6.8 ± 8.1 ng m^{-3}) and tartric (1.53 ng m^{-3} vs 1.6 ± 2.8 ng m^{-3}) acids. In contrast, malic (2.2 ng m^{-3} vs 4.9 ± 5.7 ng m^{-3}), oxalic (29.8 ng m^{-3} vs 80 ± 90 ng m^{-3}) and malonic (1.31 ng m^{-3} vs 13.8 ± 20.2 ng m^{-3}) acids were reported to be on average more abundant during the CARBOSOL project. The concentrations measured at the PUY station display intermediate values compared to those reported by Legrand et al. (2007) for the altitude sites of Schauinsland (Germany, 1205 m a.s.l.) and Vallot (French Alps, 4360 m a.s.l.). They are also in the range of the values reported by Müller et al. (2005) for the Goldauter station (605 m a.s.l.) located close to Mt Schmücke (Germany), and slightly lower than those recently measured at the same place by van Pinxteren et al. (2014).

All the species measured in the particulate phase and implemented in the initialization of the coupled model are listed in **Table 3** with their contribution to the soluble mass fraction in each mode, their molar mass and the number of ions into which they may dissociate.

3 Results and Discussion

3.1 Microphysical evolutions

Fig. 3 shows the time evolution of the simulated cloud liquid water content (LWC) and mean cloud droplet radius. It should be noted that the appearance of the cloud was scheduled around noon, when the photolysis rates are at their maximum, to favor enhanced photochemistry. Apart from the condensation and evaporation phases, the LWC is close to 0.4 g m^{-3}, with an average value of 0.3 g m^{-3} calculated from the whole simulation. A constant cloud droplet radius of 9.5 µm is obtained all along the stable phase of the cloud lifetime, between 12:20 and 13:40. These values are in good agreement with the typical values measured at the PUY station from 2001 onwards, which can be found in a database including 110 cloud events that is available online at *http://www.obs.univ-bpclermont.fr/SO/beam/data.php*. Indeed, based on this large dataset, the LWC measured at the PUY station exhibits rather limited variation, with an average value of 0.28 ± 0.12 g m^{-3}, while the droplet radius is on average approximately 10 µm (Deguillaume et al., 2014). Deguillaume et al. (2014) classified the cloud samples using a statistical analysis methodology that takes into account the physicochemical parameters of the cloud together with the back-trajectories of the sampled air masses. Cloud events in the westerly and northerly/northwesterly air masses were the most frequent, representing 72% of the air masses sampled at the PUY station, the majority of which were categorized as "Marine" or "Highly marine". The clouds sampled in the westerly/southwesterly air masses were also frequently characterized by a strong marine signature (64%). Since the aerosol particles spectrum to be activated was measured in such an air mass, the model results will be compared to the "Marine" and "Highly marine" cases classified by Deguillaume et al. (2014).

3.2 Comparison of simulated and measured in-cloud chemical concentrations - Discussion and sensitivity studies

3.2.1 Importance of particle dissolution in cloud water chemical composition

In **Table 4**, the simulated cloud water chemical concentrations are compared with those measured in "Marine" and "Highly marine" clouds observed at the PUY station (~ 70 cloud events) for a set of compounds (Deguillaume et al., 2014). The concentrations measured during "Highly marine" cases are on average higher for both inorganic and organic species compared to "Marine" ones, with also a higher pH but similar LWC. The modeled concentrations are average values calculated apart from the condensation and evaporation phases, to be close to the measuring conditions in a well-formed cloud.

The agreement between the measured and modeled hydrogen peroxide concentrations is weak. Several reasons related to measurement conditions can explain this discrepancy. In marine air masses, measured hydrogen peroxide concentration is very variable (standard deviation = 7.12 and 6.31 µM for "Highly marine" and "Marine" clouds, respectively). Additionally, during the wintertime, hydrogen the peroxide concentration is often derived from frozen samples (Marinoni et al., 2011), which can lead to an underestimation of the actual in-cloud concentration because of the outgassing of H_2O_2. In addition to measurement issues, we observed that the gas phase chemistry model used in this work (MCM) produces a large amount of H_2O_2 under our chemical scenario. The discrepancy between the observed and modeled H_2O_2 values could also arise from the presence of microorganisms, not yet considered in the model, that efficiently degrade H_2O_2 as well as formic acid (Vaïtilingom et al., 2013).

In contrast, fair agreement is found for inorganic species between the model results and observations, except for the nitrate level, which is underestimated but still in the range of measurements. Under low NO_x conditions, nitrate formation due to gas phase chemistry (mass transfer) is competing with nitrate formation through particle dissolution as seen later on (Sect. 3.3). Additionally, nitric acid is very soluble and therefore sensitive to microphysical parameters (i.e., it would be more concentrated with a lower cloud water content and smaller cloud droplets). However, despite being underestimated, the simulated nitrate concentration remains in the range of the concentrations typically measured in marine clouds.

For the di-carboxylic acids, the model predicts concentrations that are lower compared to those measured on average at the puy de Dôme. These discrepancies might, at least partly, arise from the aerosol particle spectrum used to initialize the model, which exhibited organic contents in the low range of the typical measurements. The reason for the low simulated oxalate concentrations compared to the measured ones, even when particle-to-cloud transfer is turned on, also lies in the formation of iron-oxalate complexes and their efficient photolysis. It is likely that the formation of these iron-oxalate complexes is overestimated by the model due to an incomplete coverage of the iron complexation processes with other compounds in CLEPS. The absence of competition between different ligands to form iron complexes in CLEPS leads to a high amount of free iron available to form complexes with oxalate ions, and in turn lower oxalate concentrations.

To evaluate the effect of the particle-to-cloud transfer on the cloud chemistry, a sensitivity simulation was performed without taking into account particle dissolution. The results are shown in **Table 4** (Run 2) and compared to the reference simulation (Run 1). As mentioned before, particles serving as nuclei for the formation of cloud droplets can dissolve in the cloud water and modify its chemical content. This is particularly true for ammonia and strong acids (sulfuric and nitric acids), as well as for di-carboxylic acids (oxalic, succinic and malonic acids). Indeed, particle dissolution is a major contributor of acidic content in the cloud, as highlighted by the comparison of Run 1 and Run 2 in **Table 4**: for instance, the nitrate concentration is reduced from 12 to 2.5 μM when neglecting the dissolution of particulate nitrate in the model. The effect is less obvious for sulfate because its concentration is mostly controlled by the sulfur dioxide reactivity and to a lesser extent by the dissolution of particulate sulfate, as discussed later (Sect. 3.3).

To obtain more insight into the impact of particle-to-cloud transfer on the aqueous carboxylic acid concentrations, an additional simulation was conducted. This test (Run 3) was performed using the mean particulate concentrations measured by Legrand et al. (2007) at the PUY station for oxalic, succinic, malonic, malic and tartric acids (see **supplementary material**), while all other concentrations/parameters were left unchanged when initializing the model. The concentrations provided by Legrand et al. (2007) were, however, given as a sum over the whole particle size distribution. We thus assumed that the relative contributions of each mode to the total concentration of the di-acids listed above were similar to those observed during the reference case study to calculate the distribution of these acids and further initialize the model. These relative contributions as well as the concentrations provided by Legrand et al. (2007) are provided in **Table S1** in the Supplementary material. As shown in **Fig. S2** and **Table S1**, the concentrations from Legrand et al. (2007) are higher compared to those used in Run 1, especially for oxalic, malonic and malic acids and to a lesser extent for succinic and tartric acids. **Fig. 4** presents the simulated concentrations from Runs 1 and 3 for those species.

The increased amount of organic matter in the particulate phase did not lead to a significant change in the cloud microphysical properties, which was rather determined by the dominant inorganic fraction representative of marine aerosols. In contrast, as expected, the carboxylic acid concentrations are increased in Run 3, when using data from Legrand et al. (2007), and the agreement between the modeled and measured concentrations is especially increased for oxalic and malonic acids (see Table 4). The simulated oxalate concentration is also significantly increased, and matches well with the average value representative of "Highly marine" clouds, but it remains in the lower range of "Marine" concentrations. As previously mentioned, the discrepancy between the modeled and measured oxalate concentrations might also be related to an overestimated formation of iron-oxalate complexes in the model because of some missing iron complexation processes in CLEPS. To verify this hypothesis, a new run (Run 4) was performed, similar to Run 3, i.e., with increased carboxylic acid concentrations in the particulate phase, but with the iron-oxalate chemistry turned off. However, as shown in **Fig. 5**, the iron-oxalate chemistry has a smaller influence on the oxalic acid concentration than particle-to-cloud transfer. This low sensitivity to iron-complexation chemistry may be due to the very low dissolved iron content in the cloud water ($7.6\ 10^{-2}$ μM). It can also be argued that sources of oxalic acid related to the oxidation of compounds not yet considered in the chemical mechanism are missing in the model.

Atmos. Chem. Phys. Discuss., https://doi.org/10.5194/acp-2017-699
Manuscript under review for journal Atmos. Chem. Phys.
Discussion started: 10 August 2017

Atmospheric Chemistry and Physics Discussions

3.2.3 Sensitivity study regarding cloud microphysics and acidity

A last series of tests was performed to assess the effects of other known sensitive parameters on the model results, namely the cloud liquid water content and the droplet radius (Run 5) as well as the pH (Run 6). The results of these sensitivity tests are reported in **Table 4**. Soluble species are very responsive to the cloud liquid water content and are more concentrated in the aqueous phase when the cloud droplet radius is smaller. As a consequence, most of the chemical species shown in **Table 4** display increased concentrations when the LWC and the droplet radius are both lowered (from 0.39 to 0.29 g m^{-3} and from 9.5 to 8.6 µm respectively). Additionally, the resulting pH in Run 5 is more acidic than that in Run 1.

According to Deguillaume et al. (2014), the mean pH in "Marine" clouds is 5.7, and it is 6.2 for the "Highly marine" ones (**Table 4**). The lower values obtained during Run 1 are most likely explained by the fact that for the simulation of marine air masses, the model should take into account more cations (Na^+, Mg^{2+}, K^+, Ca^{2+}). Those are currently missing in CLEPS, in which recent developments were rather focused on organic chemistry. As previously mentioned, the H^+ concentration is presently calculated in the model based on acido-basic equilibria. To further test the effect of the pH on cloud chemistry, we performed an additional run, Run 6, throughout which we imposed a pH of 6, i.e., closer to the measured values.

As shown in **Fig. 6**, increasing the pH has a great influence on weak acids, i.e., organic acids. The acetic acid concentration is much higher when the pH is less acidic, consistent with observations from the "Marine" and "Highly marine" cases. The acidic form ($CH_3CO(OH)$) is dominant as the pH is more acidic (Run 1), whereas the contribution of the anionic form ($CH_3CO(O^-)$) is increased at pH = 6 (Run 6). Both forms are produced by the reaction of pyruvic acid with hydrogen peroxide in the cloud aqueous phase, but at rates that differ significantly, being 0.12 M^{-1} s^{-1} for the acidic form ($CH_3COCO(OH)$) and 0.75 M^{-1} s^{-1} for the anionic form ($CH_3COCO(O^-)$). As a result, the total aqueous production of acetic acid is enhanced when the pH is higher. The formic acid concentration is also larger when the pH is less acidic (Run 6, **Table 4**), which is due to stronger sources mainly related to the oxidation of formaldehyde, glyoxal and glycolaldehyde by $HO^\cdot$ radicals. When the pH = 6, the $HO^\cdot$ concentration is doubled compared to that when the pH is approximately 4.3, since the decomposition of ozone by the dominant anionic form of $HO_2^\cdot$ is more efficient to produce $HO^\cdot$ radicals.

The increased $HO^\cdot$ concentration in Run 6 also affects the carboxylic acids that only come from the dissolution of aerosol particles (succinic, tartric, malic acids). They are more efficiently oxidized by the larger amount of $HO^\cdot$ radicals so that, as shown in **Fig. 6**, their concentrations decrease between Run 1 and Run 6. In the same way, oxalic acid is degraded more quickly by $HO^\cdot$ at pH = 6.

3.3 Partitioning and sources of chemical species (mass transfer from gas phase, particulate dissolution and aqueous-phase reactivity)

3.3.1 Partitioning among gas/aqueous cloud phases

In this section, the partitioning between the gas and aqueous phases is discussed in details for some species. It can be represented by a partitioning coefficient q, as introduced earlier by Chaumerliac et al. (2000):

$$q = \frac{C_{aq}(i)}{q_{cw}\, H_{eff}(i)\, RT\, C_g(i)} \qquad (17)$$

where $C_g(i)$ and $C_{aq}(i)$ are, respectively, the gaseous and aqueous concentrations of species i in molec cm^{-3}, q_{cw} is the liquid water content in vol/vol, $H_{eff}(i)$ is the Henry law effective constant of species i in M atm^{-1} and R = 0.08206 atm M^{-1} K^{-1}. This factor q indicates whether species i is at the Henry's law equilibrium (q = 1), undersaturated in the aqueous phase (q < 1) or supersaturated in the aqueous phase (q > 1).

As highlighted by Ervens (2015), the partitioning between the gas and aqueous phases cannot be described by a thermodynamic equilibrium assumption. The factor q evolves with time, as microphysical processes, mass transfer and chemical reactivity modify the partitioning of the species in the gas and aqueous phases. However, to get more insight into this partitioning, mean q values were calculated for several species over the whole cloud duration and are shown, together with their effective Henry's law constants, in **Fig. 7** for Run 1 (variable pH approximately 4.3) and Run 6 (pH = 6).

Most of the species are supersaturated in the aqueous phase (i.e., q>1), especially those with high effective Henry's law constants (i.e., larger than 10^9 $Matm^{-1}$). This is the case, for instance, for chloride and carboxylic acids, both in Runs 1 and 6, but not for sulfuric acid and nitric acid when the pH is increased (Run 6).

To complete the discussion, the q factors calculated during the different runs are shown in **Fig. 8**. Strong acids such as nitric acid or sulfuric acid are very sensitive to the cloud LWC and droplet radius, as observed when comparing Run 1 and Run 5, and they are produced more efficiently under higher pH (Run 6). Particle-to-cloud transfer is an important source of nitric acid in the cloud, and neglecting it (Run 2) leads to a strong undersaturation of nitric acid in the cloud water compared to in Run 1. In contrast, there is no difference observed between the various runs for the carboxylic acids, which essentially originate from particle dissolution.

3.3.2 Sources

The contributions of the gaseous, particulate and aqueous concentrations to the total atmospheric concentration of a given species can be evaluated from measurements within the experimental uncertainties. It is, however, difficult to evaluate by an experimental procedure how particle-to-cloud transfer, mass transfer from the gas phase and aqueous-phase reactions influence the aqueous concentrations. The model is a complementary tool that can provide such information. **Fig. 9** shows the origin of species in cloud water for Run 3. For a given compound, the contribution of each source (particulate dissolution, mass transfer from the gas phase and aqueous-phase reactivity) was calculated as the ratio of its corresponding production rate (averaged over cloud lifetime) over the total production rate.

The ammonia and formic acid molecules that are found in the aqueous phase mainly come from the gas phase, while sulfuric and acetic acids are formed through reactivity in the aqueous phase. Malonic acid exclusively originates from particle dissolution; the same applies for oxalic acid when iron-oxalate chemistry is activated. In contrast, aqueous reactivity is the major source of oxalic acid when iron complexation by oxalate are not considered As expected, C_3-C_4 carboxylic acids come mainly from particle dissolution, as shown in **Fig. 9** for malonic acid. For acetic acid, the contributions of the three sources are more equally distributed. Their relative efficiency, however, varies as a function of the pH since the production of acetic acid by aqueous-phase reactivity in the cloud water is pH-dependent. The relative contributions of the three sources to the concentration of acetic acid in cloud water are 42.3, 43 and 14.7% in Run 1 (pH approximately 4.3), while they are 34.6, 54.6 and 10.8% in Run 6 (pH = 6), for aqueous-phase reactivity, mass transfer and particle dissolution, respectively.

4 Conclusion

To describe the cloud multiphase system, the chemical model CLEPS 1.0 (Mouchel-Vallon et al., 2017), which describes the oxidation of isoprene into water-soluble organic species, has been coupled with the warm microphysical scheme module previously presented by Leriche et al. (2007). In the present study, the activation of aerosol particles into cloud droplets has been updated to account for the influence of organic surfactants (Abdul-Razzak and Ghan, 2004). Among organics, di-carboxylic acids were previously found to enhance the particles' CCN efficiency, so their contribution to the particle composition was explicitly accounted for. CLEPS 1.0 has been extended (CLEPS 1.1) to include the aqueous chemistry of these di-carboxylic acids originating from the particulate phase (succinic, malic, tartric and fumaric/maleic acids) following

the protocol described by Mouchel-Vallon et al. (2017). The new coupled model then has the ability to calculate the aqueous-phase concentrations of compounds originating from particle dissolution, mass transfer from the gas phase and the in-cloud chemical reactivity. It can also predict the partitioning of any chemical species between the gas and aqueous phases, which is not well documented by measurements, as shown in the recent review by Ervens (2015).

The present study aimed at assessing the effect of particle dissolution on the cloud water chemical content. We thus simulated the formation of a non-precipitating orographic cloud representative of those observed at the puy de Dôme from the activation of an aerosol particle spectrum characteristic of the background conditions at this site (Sellegri et al., 2003). The simulated cloud had a liquid water content of 0.4 g m^{-3} and a cloud droplet radius of 10 μm, close to the values reported by Deguillaume et al. (2014) for the so-called "Marine" and "Highly marine" cloud events (70 samples from 2011 onwards). To be consistent with the usual conditions encountered at the puy de Dôme station, the gas-phase concentrations were initialized based on low-NO_x scenario conditions in the chemistry model, as previously presented by Mouchel-Vallon et al. (2017).

The model was evaluated against the unique database built on a long-term basis at the GAW puy de Dôme station to document the cloud water chemical composition, as discussed by Deguillaume et al. (2014). The originality of the present work is to include organic species up to C_4 in the comparison between the simulated and measured concentrations; some attempts were performed in the past, but with a main focus on inorganic and short-chain organic compounds, and they were moreover often measured during short-term specific field campaigns.

The model was shown to well reproduce the inorganic levels in the cloud, with the exception of nitrate, which was underestimated because of the low-NO_x conditions. Some discrepancies were also found for H_2O_2, most likely arising from both measurement and modeling issues. The missing description of the activity of microorganisms in the model, previously reported to efficiently degrade both hydrogen peroxide and formate (Vaïtilingom et al., 2013), might also explain the overestimated concentrations of those compounds in the model.

In addition to formic acid, for the reference simulation, the model is also capable of simulating organic acid concentrations in agreement with observations, but they are on average in the lower range of the measured values reported by Deguillaume et al. (2014). Several sensitivity tests were performed to further investigate the observed discrepancies, which could finally, to a large extent, be explained by 1) an insufficient organic loading in the particle spectrum used to initialize the model and 2) significantly higher acidity in the model compared to measurements. For all these runs, the partitioning ratio is evaluated and is clearly greater than 1 (i.e., species are supersaturated in the aqueous phase), especially for soluble species (with a high effective Henry's law constant larger than 10^9 M atm^{-1}). This is related to the fact that most of the C_3-C_4 carboxylic acids come mainly from the particulate phase. Formic and acetic acids, in contrast, are more efficiently transferred from the gas phase and have a highly variable aqueous-phase reactivity depending on the cloud acidity.

Future investigations will be realized on the basis of this coupled model CLEPS 1.1 to include the effects of rain formation, ice microphysics and microbial activity on the organic chemistry in clouds.

Code availability

The mechanism used in this paper is available in KPP format upon request to l.deguillaume@opgc.univ-bpclermont.fr. Any suggestions and corrections to the mechanism (e.g., a new experimental rate constant we may have missed, typos) are also welcomed at the same address. The coupled model that was used for the simulations is also available upon request to l.deguillaume@opgc.univ-bpclermont.fr

Acknowledgments

The authors acknowledge K. Sellegri for data availability on aerosol particles and for helpful discussions. This work was supported by CEA/CNRS through contract CEA 12-27-C-DSPG/CAJ – CNRS 77265. The authors are also very grateful to the Agence Nationale de la Recherche (ANR) for its financial support through the BIOCAP project (ANR-13-BS06-0004).

References

Abbatt, J. P. D., Broekhuizen, K. and Pradeep Kumar, P.: Cloud condensation nucleus activity of internally mixed ammonium sulfate/organic acid aerosol particles, Atmos. Environ., 39(26), 4767–4778, doi:10.1016/j.atmosenv.2005.04.029, 2005.

Abdul-Razzak, H. and Ghan, S. J.: A parameterization of aerosol activation: 2. Multiple aerosol types, J. Geophys. Res. Atmospheres, 105(D5), 6837–6844, doi:10.1029/1999JD901161, 2000.

Abdul-Razzak, H. and Ghan, S. J.: Parameterization of the influence of organic surfactants on aerosol activation, J. Geophys. Res. Atmospheres, 109(D3), D03205, doi:10.1029/2003JD004043, 2004.

Abdul-Razzak, H., Ghan, S. J. and Rivera-Carpio, C.: A parameterization of aerosol activation: 1. Single aerosol type, J. Geophys. Res. Atmospheres, 103(D6), 6123–6131, doi:10.1029/97JD03735, 1998.

Asmi, E., Freney, E., Hervo, M., Picard, D., Rose, C., Colomb, A. and Sellegri, K.: Aerosol cloud activation in summer and winter at puy-de-Dôme high altitude site in France, Atmos. Chem. Phys., 12(23), 11589–11607, doi:10.5194/acp-12-11589-2012, 2012.

Berry, E. X. and Reinhardt, R. L.: An analysis of cloud drop growth by collection: Part I. Double distributions, J. Atmos. Sci., 31(7), 1814–1824, 1974a.

Berry, E.X. and Reinhardt, R.L.: An analysis of cloud drops growth by collection: Part II. Single initial distributions, J. Atmos. Sci., 31, 1825-183, 1974b.

Berry, E.X. and Reinhardt, R.L.: An analysis of cloud drops growth by collection: Part III. Accretion and self-collection, J. Atmos. Sci., 31, 2118-2126, 1974c.

Berry, E.X. and Reinhardt, R.L.: An analysis of cloud drops growth by collection: Part IV. A new parametrization, J. Atmos. Sci., 31, 2127-2135, 1974d.

Caro, D., Wobrock, W., Flossmann, A. I. and Chaumerliac, N.: A two-moment parameterization of aerosol nucleation and impaction scavenging for a warm cloud microphysics: description and results from a two-dimensional simulation, Atmos. Res., 70(3–4), 171–208, 2004.

Chaumerliac, N., Richard, E., Pinty, J.-P. and Nickerson, E. C.: Sulfur scavenging in a mesoscale model with quasi-spectral microphysics: Two-dimensional results for continental and maritime clouds, J. Geophys. Res. Atmospheres, 92(D3), 3114–3126, doi:10.1029/JD092iD03p03114, 1987.

Chebbi, A. and Carlier, P.: Carboxylic acids in the troposphere, occurrence, sources, and sinks: A review, Atmos. Environ., 30(24), 4233–4249, 1996.

Clegg, S. L., Brimblecombe, P. and Khan, I.: The Henry's law constant of oxalic acid and its partitioning into the atmospheric aerosol, Idojárás, 100(1–3), 51–68, 1996.

Corrin, M. L. and Harkins, W. D.: The effect of salts on the critical concentration for the formation of micelles in colloidal electrolytes, J. Am. Chem. Soc., 69(3), 683–688, 1947.

Dabek-Zlotorzynska, E. and McGrath, M.: Determination of low-molecular-weight carboxylic acids in the ambient air and vehicle emissions: a review, Fresenius J. Anal. Chem., 367(6), 507–518, doi:10.1007/s002160000376, 2000.

Damian, V., Sandu, A., Damian, M., Potra, F. and Carmichael, G. R.: The kinetic preprocessor KPP-a software environment for solving chemical kinetics, Comput. Chem. Eng., 26(11), 1567–1579, doi:http://dx.doi.org/10.1016/S0098-1354(02)00128-X, 2002.

Deguillaume, L., Leriche, M., Monod, A. and Chaumerliac, N.: The role of transition metal ions on HOx radicals in clouds: a numerical evaluation of its impact on multiphase chemistry, Atmos. Chem. Phys., 4(1), 95–110, doi:10.5194/acp-4-95-2004, 2004.

Deguillaume, L., Leriche, M., Desboeufs, K., Mailhot, G., George, C. and Chaumerliac, N.: Transition metals in atmospheric liquid phases: sources, reactivity, and sensitive parameters, Chem. Rev., 105(9), 3388–3431, doi:10.1021/cr040649c, 2005.

Deguillaume, L., Charbouillot, T., Joly, M., Vaïtilingom, M., Parazols, M., Marinoni, A., Amato, P., Delort, A.-M., Vinatier, V., Flossmann, A., Chaumerliac, N., Pichon, J. M., Houdier, S., Laj, P., Sellegri, K., Colomb, A., Brigante, M. and Mailhot, G.: Classification of clouds sampled at the puy de Dôme (France) based on 10 yr of monitoring of their physicochemical properties, Atmos. Chem. Phys., 14(3), 1485–1506, doi:10.5194/acp-14-1485-2014, 2014.

Djouad, R., Sportisse, B. and Audiffren, N.: Numerical simulation of aqueous-phase atmospheric models: use of a non-autonomous Rosenbrock method, Atmos. Environ., 36(5), 873–879, doi:10.1016/S1352-2310(01)00497-6, 2002.

Djouad, R., Michelangeli, D. V. and Gong, W.: Numerical solution for atmospheric multiphase models: Testing the validity of equilibrium assumptions, J. Geophys. Res. Atmospheres, 108(D19), 4602, doi:10.1029/2002JD002969, 2003.

Doussin, J.-F. and Monod, A.: Structure–activity relationship for the estimation of OH-oxidation rate constants of carbonyl compounds in the aqueous phase, Atmos. Chem. Phys., 13(23), 11625–11641, doi:10.5194/acp-13-11625-2013, 2013.

Emmerson, K. M. and Evans, M. J.: Comparison of tropospheric gas-phase chemistry schemes for use within global models, Atmos. Chem. Phys., 9(5), 1831–1845, doi:10.5194/acp-9-1831-2009, 2009.

Ervens, B.: Modeling the processing of aerosol and trace gases in clouds and fogs, Chem. Rev., 115(10), 4157–4198, doi:10.1021/cr5005887, 2015.

Ervens, B., Turpin, B. J. and Weber, R. J.: Secondary organic aerosol formation in cloud droplets and aqueous particles (aqSOA): a review of laboratory, field and model studies, Atmos. Chem. Phys., 11(21), 11069–11102, doi:10.5194/acp-11-11069-2011, 2011.

Ervens, B., Renard, P., Tlili, S., Ravier, S., Clément, J.-L. and Monod, A.: Aqueous-phase oligomerization of methyl vinyl ketone through photooxidation – Part 2: Development of the chemical mechanism and atmospheric implications, Atmos. Chem. Phys., 15(16), 9109–9127, doi:10.5194/acp-15-9109-2015, 2015.

Fountoukis, C. and Nenes, A.: Continued development of a cloud droplet formation parameterization for global climate models, J. Geophys. Res. Atmospheres, 110(D11) , doi:10.1029/2004JD005591, 2005.

Freney, E. J., Sellegri, K., Canonaco, F., Boulon, J., Hervo, M., Weigel, R., Pichon, J. M., Colomb, A., Prévôt, A. S. H. and Laj, P.: Seasonal variations in aerosol particle composition at the puy-de-Dôme research station in France, Atmos. Chem. Phys., 11(24), 13047–13059, doi:10.5194/acp-11-13047-2011, 2011.

Gelencsér and Varga: Evaluation of the atmospheric significance of multiphase reactions in atmospheric secondary organic aerosol formation, Atmos. Chem. Phys., 5(10), 2823–2831, doi:10.5194/acp-5-2823-2005, 2005.

Gérard, V., Nozière, B., Baduel, C., Fine, L., Frossard, A. A. and Cohen, R. C.: Anionic, cationic, and nonionic surfactants in atmospheric aerosols from the Baltic Coast at Askö, Sweden: Implications for cloud droplet activation, Environ. Sci. Technol., 50(6), 2974–2982, doi:10.1021/acs.est.5b05809, 2016.

Ghan, S. J., Abdul-Razzak, H., Nenes, A., Ming, Y., Liu, X., Ovchinnikov, M., Shipway, B., Meskhidze, N., Xu, J. and Shi, X.: Droplet nucleation: Physically-based parameterizations and comparative evaluation, J. Adv. Model. Earth Syst., 3(4), doi:10.1029/2011MS000074, 2011.

Herrmann, H., Schaefer, T., Tilgner, A., Styler, S. A., Weller, C., Teich, M. and Otto, T.: Tropospheric aqueous-phase chemistry: kinetics, mechanisms, and its coupling to a changing gas phase, Chem. Rev., 115(10), 4259–4334, doi:10.1021/cr500447k, 2015.

Jenkin, M. E., Young, J. C. and Rickard, A. R.: The MCM v3.3.1 degradation scheme for isoprene, Atmos. Chem. Phys., 15(20), 11433–11459, doi:10.5194/acp-15-11433-2015, 2015.

Kanakidou, M., Seinfeld, J. H., Pandis, S. N., Barnes, I., Dentener, F. J., Facchini, M. C., Dingenen, R. V., Ervens, B., Nenes, A., Nielsen, C. J. and others: Organic aerosol and global climate modelling: a review, Atmos. Chem. Phys., 5(4), 1053–1123, 2005.

Kawamura, K. and Kaplan, I. R.: Motor exhaust emissions as a primary source for dicarboxylic acids in Los Angeles ambient air, Environ. Sci. Technol., 21(1), 105–110, doi:10.1021/es00155a014, 1987.

Kawamura, K. and Sakaguchi, F.: Molecular distributions of water soluble dicarboxylic acids in marine aerosols over the Pacific Ocean including tropics, J. Geophys. Res. Atmospheres, 104(D3), 3501–3509, 1999.

Kawamura, K. and Yasui, O.: Diurnal changes in the distribution of dicarboxylic acids, ketocarboxylic acids and dicarbonyls in the urban Tokyo atmosphere, Atmos. Environ., 39(10), 1945–1960, doi:10.1016/j.atmosenv.2004.12.014, 2005.

Kawamura, K., Ono, K., Tachibana, E., Charriére, B. and Sempéré, R.: Distributions of low molecular weight dicarboxylic acids, ketoacids and α-dicarbonyls in the marine aerosols collected over the Arctic Ocean during late summer, Biogeosciences, 9(11), 4725–4737, doi:10.5194/bg-9-4725-2012, 2012.

Kawamura, K., Tachibana, E., Okuzawa, K., Aggarwal, S. G., Kanaya, Y. and Wang, Z. F.: High abundances of water-soluble dicarboxylic acids, ketocarboxylic acids and α-dicarbonyls in the mountaintop aerosols over the North China Plain during wheat burning season, Atmos. Chem. Phys., 13(16), 8285–8302, doi:10.5194/acp-13-8285-2013, 2013.

Kerminen, V.-M., Ojanen, C., Pakkanen, T., Hillamo, R., Aurela, M. and Meriläinen, J.: Low-molecular-weight dicarboxylic acids in an urban and rural atmosphere, J. Aerosol Sci., 31(3), 349–362, doi:10.1016/S0021-8502(99)00063-4, 2000.

Köhler, H.: The nucleus in and the growth of hygroscopic droplets, Trans. Faraday Soc., 32, 1152–1161, 1936.

Legrand, M., Preunkert, S., Oliveira, T., Pio, C. A., Hammer, S., Gelencsér, A., Kasper-Giebl, A. and Laj, P.: Origin of C2–C5 dicarboxylic acids in the European atmosphere inferred from year-round aerosol study conducted at a west-east transect, J. Geophys. Res. Atmospheres, 112(D23), D23S07, doi:10.1029/2006JD008019, 2007.

Leriche, M., Chaumerliac, N. and Monod, A.: Coupling quasi-spectral microphysics with multiphase chemistry: a case study of a polluted air mass at the top of the Puy de Dôme mountain (France), Atmos. Environ., 35(32), 5411–5423, doi:10.1016/S1352-2310(01)00300-4, 2001.

Leriche, M., Curier, R. L., Deguillaume, L., Caro, D., Sellegri, K. and Chaumerliac, N.: Numerical quantification of sources and phase partitioning of chemical species in cloud: application to wintertime anthropogenic air masses at the Puy de Dôme station, J. Atmospheric Chem., 57(3), 281–297, doi:10.1007/s10874-007-9073-y, 2007.

Li, Z., Williams, A. L. and Rood, M. J.: Influence of soluble surfactant properties on the activation of aerosol particles containing inorganic solute, J. Atmospheric Sci., 55(10), 1859–1866, 1998.

Lim, Y. B., Tan, Y., Perri, M. J., Seitzinger, S. P. and Turpin, B. J.: Aqueous chemistry and its role in secondary organic aerosol (SOA) formation, Atmos. Chem. Phys., 10(21), 10521–10539, 2010.

Limbeck, A. and Puxbaum, H.: Organic acids in continental background aerosols, Atmos. Environ., 33(12), 1847–1852, doi:10.1016/S1352-2310(98)00347-1, 1999.

Ludwig, J. and Klemm, O.: Organic acids in different size classes of atmospheric particulate material, Tellus B, 40(5), 340–347, 1988.

Mader, B. T., Yu, J. Z., Xu, J. H., Li, Q. F., Wu, W. S., Flagan, R. C. and Seinfeld, J. H.: Molecular composition of the water-soluble fraction of atmospheric carbonaceous aerosols collected during ACE-Asia, J. Geophys. Res. Atmospheres, 109(D6), D06206, doi:10.1029/2003JD004105, 2004.

Madronich, S. and Flocke, S.: Theoretical Estimation of Biologically Effective UV Radiation at the Earth's Surface, in Solar Ultraviolet Radiation, edited by C. S. Zerefos and A. F. Bais, pp. 23–48, Springer Berlin Heidelberg., 1997.

Marinoni, A., Parazols, M., Brigante, M., Deguillaume, L., Amato, P., Delort, A.-M., Laj, P. and Mailhot, G.: Hydrogen peroxide in natural cloud water: Sources and photoreactivity, Atmos. Res., 101(1–2), 256–263, doi:https://doi.org/10.1016/j.atmosres.2011.02.013, 2011.

McNeill, V. F., Woo, J. L., Kim, D. D., Schwier, A. N., Wannell, N. J., Sumner, A. J. and Barakat, J. M.: Aqueous-phase secondary organic aerosol and organosulfate formation in atmospheric aerosols: A modeling study, Environ. Sci. Technol., 46(15), 8075–8081, doi:10.1021/es3002986, 2012.

McNeill, V. F., Sareen, N. and Schwier, A. N.: Surface-active organics in atmospheric aerosols, in Atmospheric and Aerosol Chemistry, pp. 201–259, Springer. [online] Available from: http://link.springer.com/chapter/10.1007/128_2012_404, 2013.

Minakata, D., Li, K., Westerhoff, P. and Crittenden, J.: Development of a Group Contribution Method To Predict Aqueous Phase Hydroxyl Radical (HO•) Reaction Rate Constants, Environ. Sci. Technol., 43(16), 6220–6227, doi:10.1021/es900956c, 2009.

Mochida, M., Kawabata, A., Kawamura, K., Hatsushika, H. and Yamazaki, K.: Seasonal variation and origins of dicarboxylic acids in the marine atmosphere over the western North Pacific, J. Geophys. Res. Atmospheres, 108(D6), 4193, doi:10.1029/2002JD002355, 2003.

Monod, A. and Doussin, J. F.: Structure-activity relationship for the estimation of OH-oxidation rate constants of aliphatic organic compounds in the aqueous phase: alkanes, alcohols, organic acids and bases, Atmos. Environ., 42(33), 7611–7622, doi:10.1016/j.atmosenv.2008.06.005, 2008.

Mouchel-Vallon, C., Deguillaume, L., Monod, A., Perroux, H., Rose, C., Ghigo, G., Long, Y., Leriche, M., Aumont, B., Patryl, L., Armand, P. and Chaumerliac, N.: CLEPS 1.0: A new protocol for cloud aqueous phase oxidation of VOC mechanisms, Geo. Mod. Dev., 10(3), 1339–1362, doi:10.5194/gmd-10-1339-2017, 2017.

Müller, K., van Pinxteren, D., Plewka, A., Svrcina, B., Kramberger, H., Hofmann, D., Bächmann, K. and Herrmann, H.: Aerosol characterisation at the FEBUKO upwind station Goldlauter (II): Detailed organic chemical characterisation, Atmos. Environ., 39(23–24), 4219–4231, doi:10.1016/j.atmosenv.2005.02.008, 2005.

Nenes, A., Ghan, S., ABDUL-RAZZAK, H., Chuang, P. Y. and Seinfeld, J. H.: Kinetic limitations on cloud droplet formation and impact on cloud albedo, Tellus B, 53(2), 133–149, 2001.

Nozière, B., Baduel, C. and Jaffrezo, J.-L.: The dynamic surface tension of atmospheric aerosol surfactants reveals new aspects of cloud activation, Nat. Commun., 5, 3335, doi:10.1038/ncomms4335, 2014.

Phinney, L. A., Lohmann, U. and Leaitch, W. R.: Limitations of using an equilibrium approximation in an aerosol activation parameterization, J. Geophys. Res. Atmospheres, 108(D12), 4371, doi:10.1029/2002JD002391, 2003.

van Pinxteren, D., Neusüß, C. and Herrmann, H.: On the abundance and source contributions of dicarboxylic acids in size-resolved aerosol particles at continental sites in central Europe, Atmos. Chem. Phys., 14(8), 3913–3928, doi:10.5194/acp-14-3913-2014, 2014.

van Pinxteren, D., Fomba, K. W., Mertes, S., Müller, K., Spindler, G., Schneider, J., Lee, T., Collett, J. L. and Herrmann, H.: Cloud water composition during HCCT-2010: Scavenging efficiencies, solute concentrations, and droplet size \hack\newlinedependence of inorganic ions and dissolved organic carbon, Atmos. Chem. Phys., 16(5), 3185–3205, doi:10.5194/acp-16-3185-2016, 2016.

Prisle, N. L., Asmi, A., Topping, D., Partanen, A.-I., Romakkaniemi, S., Dal Maso, M., Kulmala, M., Laaksonen, A., Lehtinen, K. E. J., McFiggans, G. and Kokkola, H.: Surfactant effects in global simulations of cloud droplet activation, Geophys. Res. Lett., 39(5), L05802, doi:10.1029/2011GL050467, 2012.

Raventos-Duran, T., Camredon, M., Valorso, R., Mouchel-Vallon, C. and Aumont, B.: Structure-activity relationships to estimate the effective Henry's law constants of organics of atmospheric interest, Atmos. Chem. Phys., 10(16), 7643–7654, doi:10.5194/acp-10-7643-2010, 2010.

Renard, P., Siekmann, F., Salque, G., Demelas, C., Coulomb, B., Vassalo, L., Ravier, S., Temime-Roussel, B., Voisin, D. and Monod, A.: Aqueous-phase oligomerization of methyl vinyl ketone through photooxidation – Part 1: Aging processes of oligomers, Atmos. Chem. Phys., 15(1), 21–35, doi:10.5194/acp-15-21-2015, 2015.

Rogge, W. F., Hildemann, L. M., Mazurek, M. A. and Cass, G. R.: Sources of fine organic aerosol. 9. Pine, oak, and synthetic log combustion in residential fireplaces, Environ. Sci. Technol., 32(1), 13–22, doi:10.1021/es960930b, 1998.

Saunders, S. M., Pascoe, S., Johnson, A. P., Pilling, M. J. and Jenkin, M. E.: Development and preliminary test results of an expert system for the automatic generation of tropospheric VOC degradation mechanisms, Atmos. Environ., 37(13), 1723–1735, doi:10.1016/S1352-2310(03)00072-4, 2003.

Saxena, P. and Hildemann, L. M.: Water-soluble organics in atmospheric particles: A critical review of the literature and application of thermodynamics to identify candidate compounds, J. Atmos. Chem., 24(1), 57–109, doi:10.1007/BF00053823, 1996.

Schwartz, S. E.: Mass-transport considerations pertinent to aqueous phase reactions of gases in liquid-water clouds, in Chemistry of Multiphase Atmospheric Systems, edited by D. W. Jaeschke, pp. 415–471, Springer Berlin Heidelberg., 1986.

Sellegri, K., Laj, P., Peron, F., Dupuy, R., Legrand, M., Preunkert, S., Putaud, J.-P., Cachier, H. and Ghermandi, G.: Mass balance of free tropospheric aerosol at the Puy de Dôme (France) in winter, J. Geophys. Res. Atmospheres, 108(D11), 4333, doi:10.1029/2002JD002747, 2003.

Sempére, R. and Kawamura, K.: Comparative distributions of dicarboxylic acids and related polar compounds in snow, rain and aerosols from urban atmosphere, Atmos. Environ., 28(3), 449–459, 1994.

Shulman, M. L., Jacobson, M. C., Carlson, R. J., Synovec, R. E. and Young, T. E.: Dissolution behavior and surface tension effects of organic compounds in nucleating cloud droplets, Geophys. Res. Lett., 23(3), 277–280, 1996.

Simpson, E., Connolly, P. and McFiggans, G.: An investigation into the performance of four cloud droplet activation parameterisations, Geo. Mod. Dev., 7(4), 1535–1542, doi:10.5194/gmd-7-1535-2014, 2014.

Sullivan, A. P., Hodas, N., Turpin, B. J., Skog, K., Keutsch, F. N., Gilardoni, S., Paglione, M., Rinaldi, M., Decesari, S., Facchini, M. C., Poulain, L., Herrmann, H., Wiedensohler, A., Nemitz, E., Twigg, M. M. and Collett, J. L.: Evidence for ambient dark aqueous SOA formation in the Po Valley, Italy, Atmos. Chem. Phys., 16, 8095-8108, 2016.

Szyskowski, B.: Experimentelle Studien über kapillare Eigenschaften der wasserigen Losungen von Fettsauren, Z. Phys. Chem., 64, 385–414, 1908.

Vaïtilingom, M., Deguillaume, L., Vinatier, V., Sancelme, M., Amato, P., Chaumerliac, N. and Delort, A.-M.: Potential impact of microbial activity on the oxidant capacity and organic carbon budget in clouds, Proc. Natl. Acad. Sci., 110(2), 559–564, doi:10.1073/pnas.1205743110, 2013.

Yao, X., Fang, M. and Chan, C. K.: Size distributions and formation of dicarboxylic acids in atmospheric particles, Atmos. Environ., 36(13), 2099–2107, doi:10.1016/S1352-2310(02)00230-3, 2002.

Zobrist, B., Marcolli, C., Koop, T., Luo, B. P., Murphy, D. M., Lohmann, U., Zardini, A. A., Krieger, U. K., Corti, T., Cziczo, D. J., Fueglistaler, S., Hudson, P. K., Thomson, D. S. and Peter, T.: Oxalic acid as a heterogeneous ice nucleus in the upper troposphere and its indirect aerosol effect, Atmos. Chem. Phys., 6(10), 3115–3129, doi:10.5194/acp-6-3115-2006, 2006.

Atmos. Chem. Phys. Discuss., https://doi.org/10.5194/acp-2017-699
Manuscript under review for journal Atmos. Chem. Phys.
Discussion started: 10 August 2017

Atmospheric Chemistry and Physics Discussions

Table 1: Initial gas phase concentrations, emission and deposition rates adapted from McNeill et al. (2012).

	Initial concentration (ppb)	Emission (molec cm^{-3} s^{-1})	Deposition (s^{-1})
SO_2	1	2.91×10^{5}	5×10^{-5}
NO	-	2.86×10^{5}	-
NO_2	0.3	-	4×10^{-6}
N_2O_5	-	-	2×10^{-5}
HNO_3	0.3	-	2×10^{-5}
O_3	40	-	4×10^{-6}
H_2O_2	1	-	1×10^{-4}
CH_4	1.7×10^{3}	-	-
CO_2	3.6×10^{5}	-	-
CO	1.5×10^{2}	3.7×10^{6}	1×10^{-6}
Isoprene	1	4.50×10^{6} [a]	-
Dihydroxybutanone	-	-	1×10^{-5}
MACR	-	-	1×10^{-5}
MVK	-	-	1×10^{-5}
Glyoxal	0.1	-	1×10^{-5}
Methylglyoxal	0.1	-	1×10^{-5}
Glycolaldehyde	-	-	1×10^{-5}
Acetaldehyde	0.1	3.17×10^{3}	1×10^{-5}
Formaldehyde	0.5	3.03×10^{3}	1×10^{-5}
Acetone	0.1	8.92×10^{3}	1×10^{-5}
Pyruvic Acid	-	-	1×10^{-5}
Acetic Acid	1×10^{-3}	3.35×10^{3}	1×10^{-5}
Formic Acid	-	-	1×10^{-5}
Methanol	2	1.07×10^{4}	1×10^{-5}
Methylhydroperoxide	0.01	3.35×10^{3}	1×10^{-5}

[a] = 0 at night time

Atmos. Chem. Phys. Discuss., https://doi.org/10.5194/acp-2017-699
Manuscript under review for journal Atmos. Chem. Phys.
Discussion started: 10 August 2017

Atmospheric Chemistry and Physics Discussions

Table 2: Physical properties of aerosol particles. For each mode N_{ap} is the particle concentration, d_{apm} is the median diameter, σ is the geometric standard deviation, ρ_{ap} is the density of aerosols and ε is the soluble fraction of the mode.

Mode	N_{ap} (cm^{-3})	d_{apm} (μm)	log σ	ρ_{ap} ($g\ cm^{-3}$)	ε (%)
1	111.9	0.076	0.255	1.62	46.0
2	4.2	0.410	0.278	1.67	63.3
3	1.5	0.660	0.041	1.73	78.8
4	0.026	2.6	0.301	1.71	77.3

Atmos. Chem. Phys. Discuss., https://doi.org/10.5194/acp-2017-699
Manuscript under review for journal Atmos. Chem. Phys.
Discussion started: 10 August 2017

Atmospheric Chemistry and Physics Discussions

Table 3: Chemical composition of aerosol particles. Each species is given with its contribution to the soluble mass in each mode (ε_{spc}), its molar mass (M_{spc}) and the number of ions into which it may dissociate (ν_{spc}).

	ε_{spc} (%)				ν_{spc}	M_{spc} (g mol^{-1})
	Mode 1	Mode 2	Mode 3	Mode 4		
NO_3^-	1.39 10^1	1.58 10^1	1.58 10^1	2.73 10^1	1	62.0
NH_4^+	6.96	1.72 10^1	2.77 10^1	1.01	1	18.0
SO_4^{2-}	1.66 10^1	2.65 10^1	3.96 10^1	2.18 10^1	2	96.0
Na^+	1.24	3.86 10^{-1}	9.44 10^{-1}	1.80 10^1	1	23.0
Cl^-	4.11	2.97 10^{-1}	2.27 10^{-1}	6.15	1	35.5
Iron [(a)]	0.00	6.93 10^{-2}	1.40 10^{-1}	3.38 10^{-1}	1	73.0
Formate	4.15 10^{-1}	4.12 10^{-1}	5.38 10^{-1}	2.47	1	46.0
Oxalate	3.65 10^{-1}	1.19	1.21	2.23	1	88.0
Acetate	1.38	1.38 10^{-1}	8.43 10^{-2}	1.47	1	59.0
Glycolate	2.15 10^{-1}	1.16 10^{-1}	7.58 10^{-2}	1.26 10^{-1}	1	75.0
Glyoxylate	1.22 10^{-1}	5.66 10^{-2}	1.40 10^{-1}	2.06 10^{-1}	1	73.0
Lactate	1.23 10^1	4.72	1.93	7.19	1	89.0
Propionate	1.87 10^{-1}	2.27 10^{-1}	2.22 10^{-1}	3.88 10^{-1}	1	73.0
Malonate	0.00	2.09 10^{-2}	7.28 10^{-2}	7.40 10^{-2}	2	103.0
Succinate	2.82 10^{-1}	2.59 10^{-1}	2.06 10^{-1}	3.72 10^{-1}	2	117.0
Malate	0.00	1.08 10^{-1}	1.28 10^{-1}	2.80 10^{-2}	2	133.0
Tartrate	0.00	4.43 10^{-2}	5.18 10^{-2}	1.34 10^{-1}	2	149.0

[(a)] An iron solubility of 15% was assumed according to Deguillaume et al. (2005).

Atmos. Chem. Phys. Discuss., https://doi.org/10.5194/acp-2017-699
Manuscript under review for journal Atmos. Chem. Phys.
Discussion started: 10 August 2017

Atmospheric Chemistry and Physics Discussions

Table 4: Chemical concentrations, pH, and cloud liquid water content (LWC) measured in clouds sampled at the puy de Dôme and calculated by the model during the 6 different runs. Main characteristic settings are recalled for each run, and colors introduce the color code used in all figures throughout the paper.

	Observations						**Model simulations**					
	« Marine »			**« Highly marine »**								
Concentration (µM)	Mean	Min	Max	Mean	Min	Max	**Run 1** ***Reference***	Run 2 *No particle dissolution*	Run 3 *Increased amount of organics in particle phase*	Run 4 *Formation of iron oxalate complexes turned off*	Run 5 *Decreased cloud liquid water content and droplet radius*	Run 6 *pH = 6*
H_2O_2	**6.2**	0.1	20.8	**11.2**	0.8	19	**65.22**	63.17	75.45	64.96	78.71	71.85
Ammonium	**43.2**	6	96.2	**88.4**	28.6	219.6	**61.80**	47.62	60.74	60.76	80.97	56.65
Sulfate	**14.15**	1.95	38.6	**39.65**	9.4	130.8	**37.31**	29.99	36.70	36.70	49.13	37.31
Nitrate	**24.8**	0.8	93.2	**59.3**	9.7	231.8	**11.96**	2.48	11.12	11.12	15.88	11.96
Formate	**6.3**	0.8	29	**13**	2.3	42.4	**20.52**	19.83	20.56	20.46	23.59	25.84
Acetate	**4.9**	0.3	22.2	**12**	1.8	57.6	**3.41**	3.31	3.42	3.39	3.45	12.50
Oxalate	**2.1**	0.2	7.5	**3.6**	1.5	12	**0.49**	0.05	2.32	2.55	0.64	0.47
Succinate	**0.6**		3.5	**1.1**	0	4.5	**0.06**	0	0.15	0.15	0.09	0.06
Malonate	**0.7**	0.3	2.9	**1.1**	0.3	3.9	**0.02**	$1.4\ 10^{-11}$	0.42	0.42	0.02	0.02
LWC ($g\ m^{-3}$)	**0.28**			**0.27**			**0.39**				0.29	
pH	**5.7**	4.6	7.6	**6.2**	4.7	6.9	**4.37**	4.36	4.38	4.36	4.29	6.00

Atmos. Chem. Phys. Discuss., https://doi.org/10.5194/acp-2017-699
Manuscript under review for journal Atmos. Chem. Phys.
Discussion started: 10 August 2017

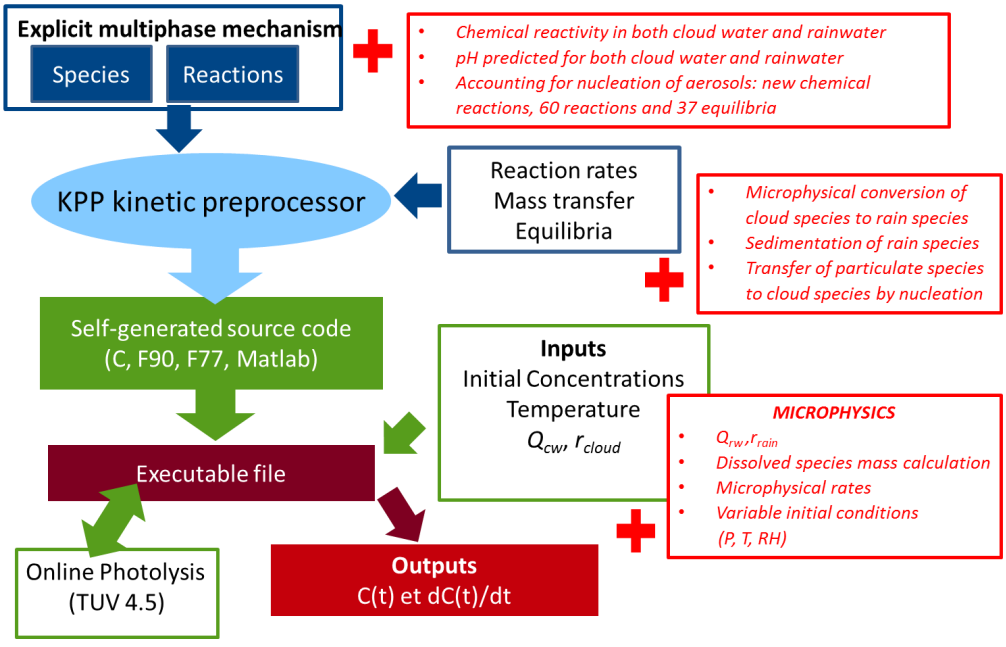

Figure 1: Schematic diagram of CLEPS (Mouchel-Vallon et al., 2017). The developments related to the coupling of CLEPS with the microphysical scheme are shown in red.

Atmos. Chem. Phys. Discuss., https://doi.org/10.5194/acp-2017-699
Manuscript under review for journal Atmos. Chem. Phys.
Discussion started: 10 August 2017

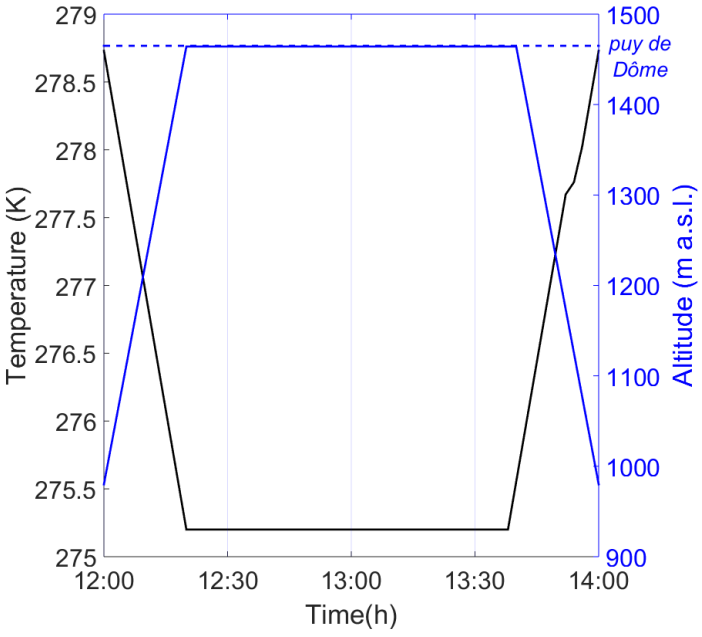

Figure 2: Temperature and altitude profiles prescribed to simulate the occurrence of a non-precipitating orographic cloud at the top of puy de Dôme mountain.

Atmos. Chem. Phys. Discuss., https://doi.org/10.5194/acp-2017-699
Manuscript under review for journal Atmos. Chem. Phys.
Discussion started: 10 August 2017

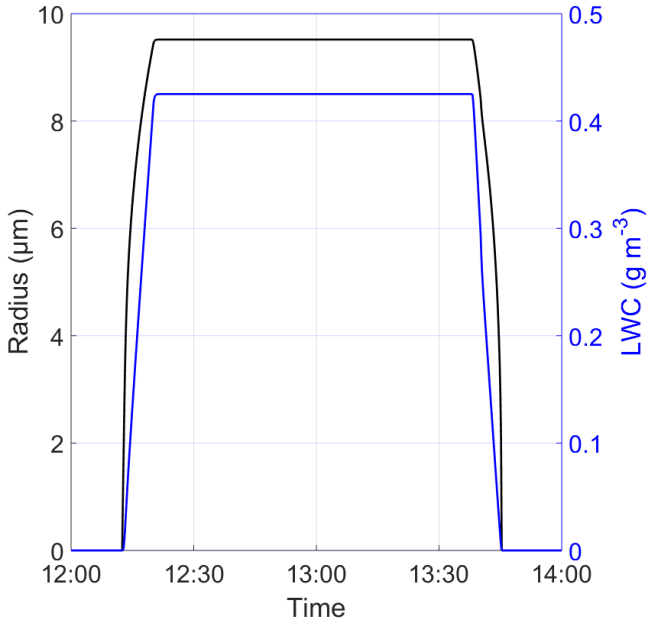

Figure 3: Time evolution of the mean cloud droplet radius (left axis) and cloud liquid water content (right axis).

Atmos. Chem. Phys. Discuss., https://doi.org/10.5194/acp-2017-699
Manuscript under review for journal Atmos. Chem. Phys.
Discussion started: 10 August 2017

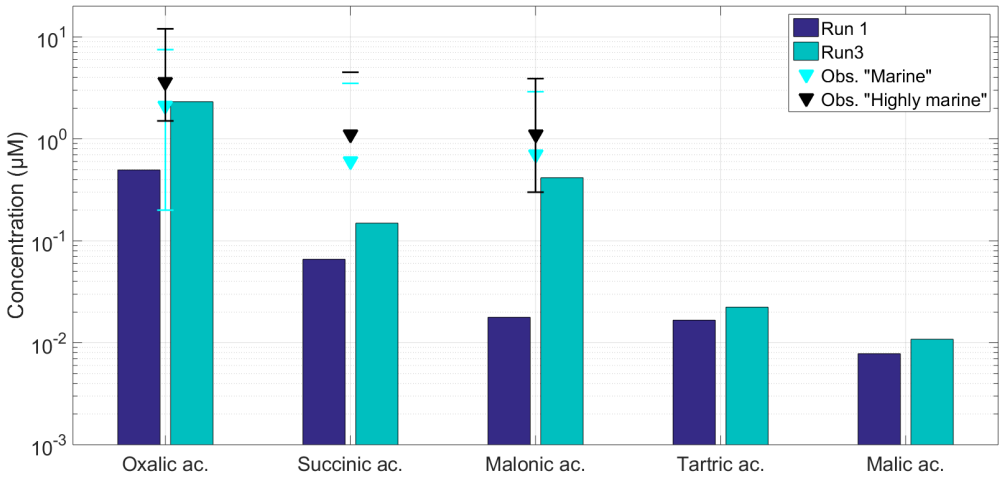

Figure 4: Averaged concentrations of some carboxylic acids calculated by the model during Run 1 (reference) and Run 3 (increased amount of organics in the particle phase). When available, the concentrations measured in "Marine" and "Highly marine" clouds sampled at the puy de Dôme and reported by Deguillaume et al. (2014) are shown for comparison. Markers represent the mean concentrations, while lower and upper limits of the error bars respectively show the minimum and maximum concentrations measured at this site. For succinic acid, minimum concentration was below the detection limit of the instrument and is thus not shown.

Atmos. Chem. Phys. Discuss., https://doi.org/10.5194/acp-2017-699
Manuscript under review for journal Atmos. Chem. Phys.
Discussion started: 10 August 2017

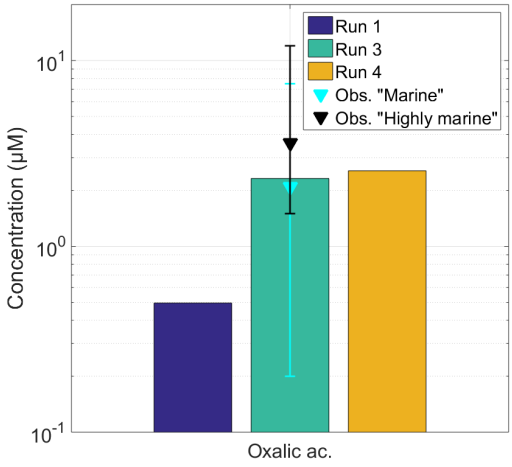

Figure 5: Averaged concentrations of oxalic acid calculated by the model during Run 1 (reference), Run 3 (increased amount of organics in the particle phase) and Run 4 (same as Run 3 but with formation of iron oxalate complexes turned off). Concentrations measured in "Marine" and "Highly marine" clouds sampled at the puy de Dôme (Deguillaume et al., 2014) are reported for comparison. Markers represent the mean concentrations, while lower and upper limits of the error bars respectively show the minimum and maximum concentrations measured at this site.

Atmos. Chem. Phys. Discuss., https://doi.org/10.5194/acp-2017-699
Manuscript under review for journal Atmos. Chem. Phys.
Discussion started: 10 August 2017

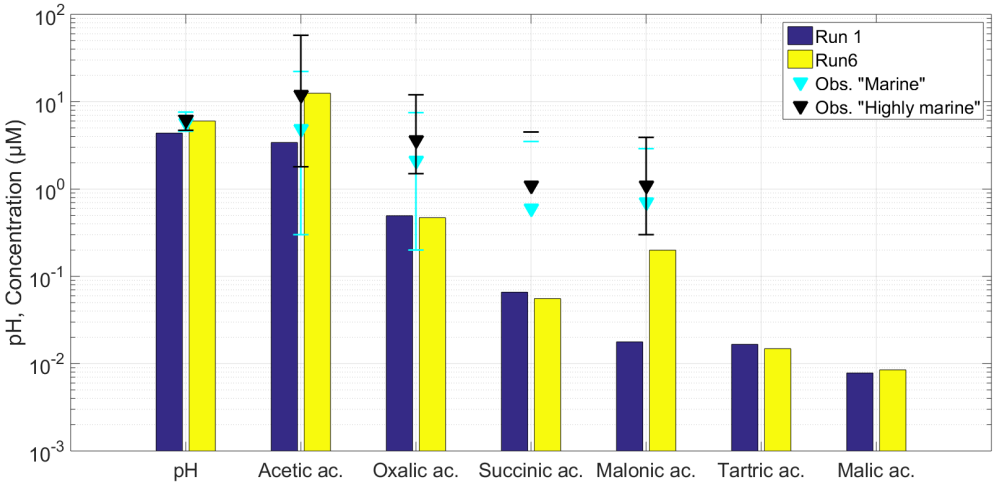

Figure 6: Averaged concentrations of some carboxylic acids calculated by the model during Run 1 (reference) and Run 6 (pH = 6). When available, the concentrations measured in "Marine" and "Highly marine" clouds sampled at the puy de Dôme and reported by Deguillaume et al. (2014) are shown for comparison. Markers represent the mean concentrations, while lower and upper limits of the error bars respectively show the minimum and maximum concentrations measured at this site. For succinic acid, minimum concentration was below the detection limit of the instrument and is thus not shown.

Atmos. Chem. Phys. Discuss., https://doi.org/10.5194/acp-2017-699
Manuscript under review for journal Atmos. Chem. Phys.
Discussion started: 10 August 2017

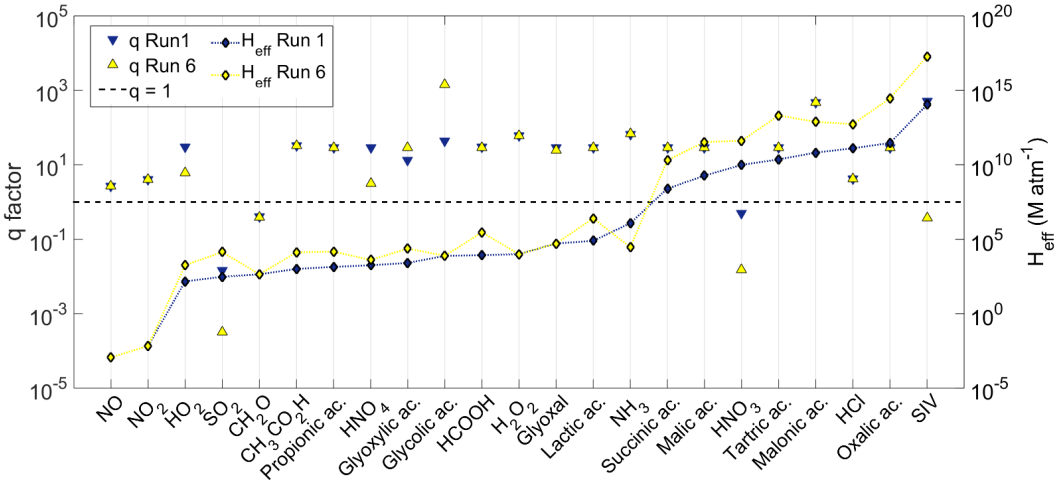

Figure 7: Effective Henry's law constant (H_{eff}) and partitioning coefficient q calculated for a selection of compounds during Runs 1 (reference) and 6 (pH = 6). Data for effective Henry's law constants are artificially linked with dashed lines for more clarity.

Atmos. Chem. Phys. Discuss., https://doi.org/10.5194/acp-2017-699
Manuscript under review for journal Atmos. Chem. Phys.
Discussion started: 10 August 2017

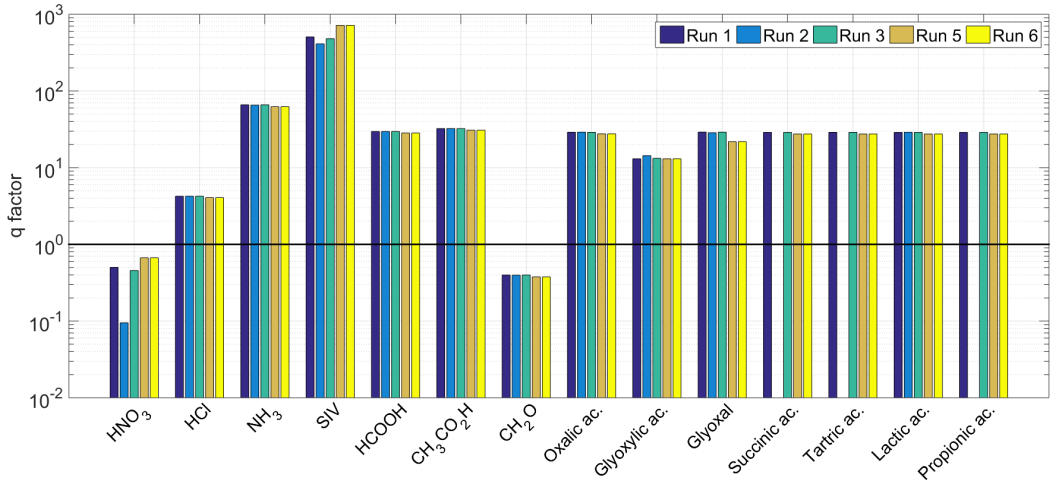

Figure 8: Partitioning coefficients q (log scale) calculated for a selection of compounds during Run 1 (reference), Run 2 (no particle dissolution), Run 3 (increased amount of organics in the particle phase), Run 5 (decreased cloud liquid water content and droplet radius) and Run 6 (pH = 6).

Atmos. Chem. Phys. Discuss., https://doi.org/10.5194/acp-2017-699
Manuscript under review for journal Atmos. Chem. Phys.
Discussion started: 10 August 2017

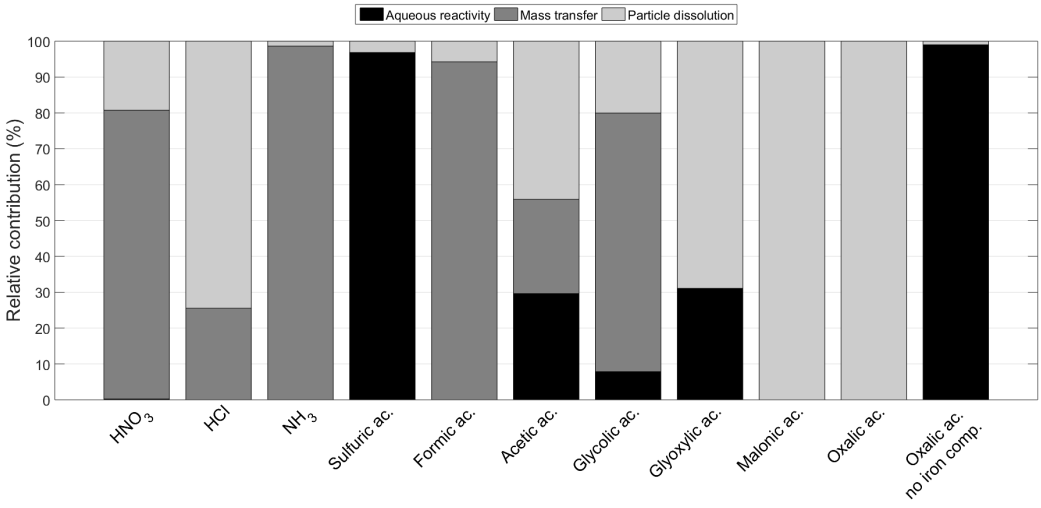

Figure 9: Relative contributions of particle dissolution, mass transfer and aqueous reactivity to the production of selected compounds during Run 3 (increased amount of organics in the particle phase).